

# Novel compact single-band and dual-band bandpass filter based on one-third-mode substrate integrated waveguide

Sheng Zhang<sup>1a)</sup>, Jia-Yu Rao<sup>1</sup>, Jun-Jie Cheng<sup>1</sup>, Xue-Dong Fu<sup>1</sup>, Fa-Lin Liu<sup>2</sup>, and Jia-Sheng Hong<sup>3</sup>

<sup>1</sup> School of Information and Control Engineering, China University of Mining and Technology, XuZhou, 221116, China

<sup>2</sup> Department of Electronic Engineering and Information Science, University of Science and Technology of China, Hefei, 230027, China

<sup>3</sup> Department of Electrical, Electronic and Computer Engineering, Heriot-Watt University, Edinburgh EH14 4AS, UK

a) [zhangsheng@cumt.edu.cn](mailto:zhangsheng@cumt.edu.cn)

**Abstract:** In this paper, a novel structure of One-Third-Mode Substrate Integrated Waveguide Resonator (OTMSIWR) is first proposed, which reduces about 65% size. Based on the OTMSIWR, a single-band bandpass filter (BPF) operates at 4.55 GHz is designed. The single-band BPF has a wide and deep upper stopband. Further, a dual-band BPF using high mode technology based on the single-band filter is designed. The fundamental mode ( $TM_{101}$  mode) and high mode ( $TM_{201}$  mode) are utilized to achieve the dual-band response. The center frequencies locate at the 4.2 GHz and 6.15 GHz, respectively. Two transmission zeros (TZs) are achieved in the dual-band BPF by adjusting the positions of the feeds. To further improve the selectivity of the upper stopband of the dual-band BPF, two pairs of Complementary Split-Ring Resonators (CSRRLs) are introduced on the surface of the OTMSIWR, which obtain the desired results. Finally, a single-band BPF and a dual-band BPF are fabricated and tested. The measured results agreed well with the simulated ones, which proved that the proposed structure is a good candidate to design filters.

**Keywords:** single-band BPF, dual-band BPF, dual-mode

**Classification:** Microwave and millimeter-wave devices, circuits, and modules

## References

- [1] D. Deslandes and K. Wu: "Single-substrate integration technique of planar circuits and waveguide filters," *IEEE Trans. Microw. Theory Techn.* **51** (2003) 593 (DOI: [10.1109/TMTT.2002.807820](https://doi.org/10.1109/TMTT.2002.807820)).

- [2] A. Sahu, *et al.*: “Recent advances in theory and applications of substrate-integrated waveguides: A review,” *Int. J. RF Microw. Comput.-Aided Eng.* **26** (2016) 129 (DOI: [10.1002/mmce.20946](https://doi.org/10.1002/mmce.20946)).
- [3] S. S. Sabri, *et al.*: “A review of substrate integrated waveguide (SIW) bandpass filter based on different method and design,” 2012 IEEE Asia-Pacific Conference on Applied Electromagnetics (APACE) (2012) 210 (DOI: [10.1109/APACE.2012.6457662](https://doi.org/10.1109/APACE.2012.6457662)).
- [4] H. Y. Chien, *et al.*: “Miniaturized bandpass filters with double-folded substrate integrated waveguide resonators in LTCC,” *IEEE Trans. Microw. Theory Techn.* **57** (2009) 1774 (DOI: [10.1109/TMTT.2009.2022591](https://doi.org/10.1109/TMTT.2009.2022591)).
- [5] V. Sekar and K. Entesari: “A novel compact dual-band half-mode substrate integrated waveguide bandpass filter,” 2011 IEEE MTT-S International Microwave Symposium Digest (MTT) (2011) 1 (DOI: [10.1109/MWSYM.2011.5972733](https://doi.org/10.1109/MWSYM.2011.5972733)).
- [6] X. Zhang, *et al.*: “Design of compact dual-passband LTCC filter exploiting stacked QMSIW and EMSIW,” *Electron. Lett.* **51** (2015) 912 (DOI: [10.1049/el.2015.0391](https://doi.org/10.1049/el.2015.0391)).
- [7] Y. C. Li, *et al.*: “Dual-mode dual-band bandpass filter based on a stub-loaded patch resonator,” *IEEE Microw. Wireless Compon. Lett.* **21** (2011) 525 (DOI: [10.1109/LMWC.2011.2164394](https://doi.org/10.1109/LMWC.2011.2164394)).
- [8] K. S. Chin, *et al.*: “Compact dual-band bandstop filters using stepped-impedance resonators,” *IEEE Microw. Wireless Compon. Lett.* **17** (2007) 849 (DOI: [10.1109/LMWC.2007.910481](https://doi.org/10.1109/LMWC.2007.910481)).
- [9] X. P. Chen, *et al.*: “Dual-band and triple-band substrate integrated waveguide filters with Chebyshev and quasi-elliptic responses,” *IEEE Trans. Microw. Theory Techn.* **55** (2007) 2569 (DOI: [10.1109/TMTT.2007.909603](https://doi.org/10.1109/TMTT.2007.909603)).
- [10] K. Wang, *et al.*: “A novel compact dualband filter based on quartermode substrate integrated waveguide and complementary splitting resonator,” *Microw. Opt. Technol. Lett.* **58** (2016) 2704 (DOI: [10.1002/mop.30131](https://doi.org/10.1002/mop.30131)).
- [11] K. Wang, *et al.*: “A novel SIW dualband bandpass filter on a doublelayer substrate using loaded posts,” *Microw. Opt. Technol. Lett.* **58** (2016) 155 (DOI: [10.1002/mop.29511](https://doi.org/10.1002/mop.29511)).

## 1 Introduction

Bandpass filters (BPFs) with high performance, low cost are playing a crucial role in modern radio frequency circuits. In order to meet these needs, Substrate Integrate Waveguide (SIW) technology is proposed and utilized to design various high-quality BPFs owing to their high Q value, low cost and easy integration with planar circuits [1, 2, 3]. However, SIW is still large, especially at designing of lower frequency microwave BPFs. To fulfill the SIW BPFs miniaturization, half-mode SIW, folded half-mode SIW and quarter-mode SIW have been widely used for designing filters with size reduction [4, 5, 6].

Dual-band BPFs are indispensable components in modern communication systems. So far, most of the dual-band BPFs are using patch resonators [7] and stepped-impedance resonators (SIR) [8]. But there are few works to design the dual BPFs using SIW. In [9], a synthesis technique is developed to design a dual-band and a triple-band filter, but the sizes of the filters are large. A miniaturized dual-band BPF is designed in [10], but it has a poor performance at the outside of the

passband. In [11], double-layer substrate is utilized to fulfill dual-band response, but it costs much.

In this paper, a novel OTMSIWR is proposed firstly. Based on it, a compact single-band BPF is designed, which reduces about 65% size compared with the same frequency filters of standard triangle SIW. Two OTMSIWRs with inductive windows are utilized for the single-band BPF to fulfill filter response and compact size. Slots are etched on the surface of the waveguide to obtain the desired coupling strength. The fabricated single-band BPF operates at 4.55 GHz with a wide and deep upper stopband from 5 GHz to 11 GHz. Further, based on the single band filter, a dual-band BPF is designed. Another two inductive windows are used to make the  $TM_{201}$  mode couple with each other, then it achieves the second-passband response. For the dual-band BPF, two TZs are obtained by adjusting the locations of the feeds, and CSRRs are applied to further improve the inhibition performance of the upper stopband. The final measured results exhibits a stopband suppression better than 40 dB around the filter passbands.

## 2 Analysis of the OTMSIWR resonator

Fig. 1 shows the structure of the novel OTMSIWR resonator, which is generated by trisecting equilateral triangle from the center of gravity to the bottom corner to do bisector. According to [10] and by means of least square method, the resonant frequency of the fundamental mode can be calculated as follows,

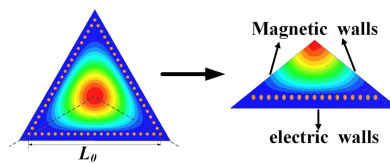
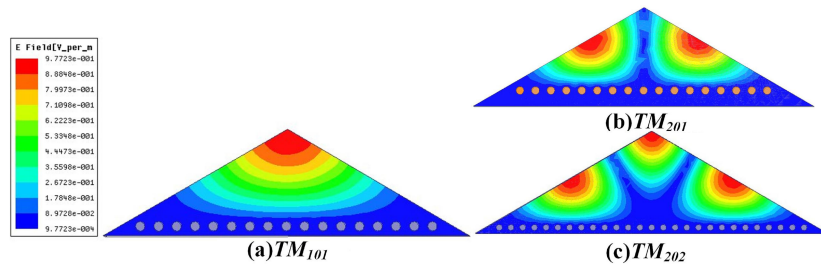


Fig. 1. Process of evolution from SIWR to OTMSIWR

$$f \approx \frac{c}{\sqrt{\epsilon_r \times \mu_r}} \times \frac{1.24}{L_0} \quad (1)$$

Where  $c$  is velocity of light in the vacuum,  $\mu_r$  and  $\epsilon_r$  are relative permeability and permittivity of the substrate,  $L_0$  is the side length of the OTMSIWR. Fig. 2 depicts the electric field distributions of the  $TM_{101}$  mode,  $TM_{201}$  mode and  $TM_{202}$  mode. And the eigen-mode frequency are 5.04 GHz, 8.03 GHz, 10.07 GHz, respectively. It can be found that the electric field characteristic of the  $TM_{101}$  mode of the OTMSIWR is similar to the SIW resonator in Fig. 2(a). Meantime, the unloaded quality factor ( $Q_u$ ) of the  $TM_{101}$  mode of the OTMSIWR is shown in Table I. The  $Q_{u-OTMSWR}$  is a little lower than  $Q_{u-SIWR}$  while size reduces 65%. So it is a competitive candidate for filters miniaturization. In Fig. 2(b), a virtual electric wall exists in the center of the resonator while the electric field strength of the  $TM_{101}$  mode is maximum. Hence, based on the feature and by selecting the suitable coupling method, the  $TM_{101}$  mode can be coupled with each other while  $TM_{102}$  mode and  $TM_{201}$  mode can be inhibited.



**Fig. 2.** The electric field distributions of the fundamental mode and high mode of the OTMSIWR

**Table I.** Resonant frequency and  $Q_u$  of OTMSIWR and SIWR

$L_0$ (mm)	$f_0$ (GHz)	$Q_{u-SIWR}$	$Q_{u-OTMSIWR}$
30	5.04	258.2	220.9
25	6.14	313.2	269.6
20	7.88	398.5	345.7
15	10.96	545.9	481.2

### 3 Filter design

#### 3.1 Single-band BPF design

To demonstrate the application of the proposed OTMSIWR, a single band BPF is designed as shown in Fig. 3. Two OTMSIWRs are cascaded with inductive window. By adjusting the width of inductive window ( $L_1$ ), the  $TM_{201}$  mode and  $TM_{202}$  mode can be significantly inhibited. Then, a wide and deep upper stopband will be appeared. Moreover, slot coupling is employed to enhance coupling strength of the fundamental mode between the two OTMSIWR cavities. By adjusting the parameters  $L_{S1}$ ,  $L_{S2}$  simultaneously, the desired coupling coefficient can be obtained with the width of the slot is 0.2 mm. The substrate used in this paper is *RT/duroid 6006*,  $\epsilon_r = 6.15$ ,  $\tan\delta = 0.0019$  and thickness  $h = 0.635$  mm. According to Eq. (1), the size of the OTMSIWR cavity centred at 4.55 GHz can be calculated. The I/O feed lines are  $50\Omega$  microstrip line. The final dimensions are as follows (unit:mm):  $L_0 = 20$ ,  $d = 0.5$ ,  $P = 1.0$ ,  $L_{S0} = 4.0$ ,  $W_{S0} = 0.95$ ,  $L_{S1} = 1.43$ ,  $L_{S2} = 0.39$ ,  $L_1 = 4.42$ .

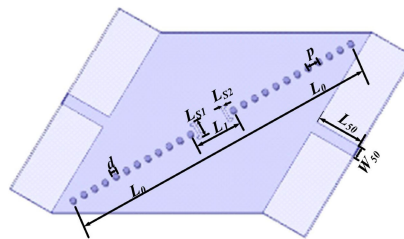


**Fig. 3.** Structure of the single-band BPF

In Fig. 4, the measured central frequency is 4.55 GHz, and the 3 dB bandwidth is 300 MHz. The insertion loss  $S_{21}$  is 2.28 dB, which is a little larger than the

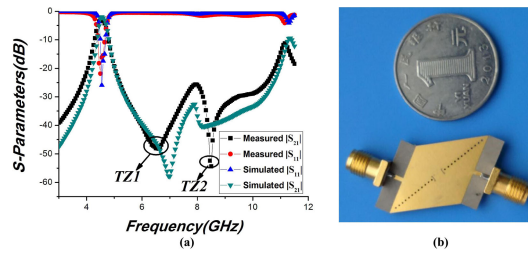


Fig. 4. (a) S-parameters (b) Photograph of the BPF

simulated one as the radiation loss at the open corner and unavoidable tolerance in fabrication and measurement. Two TZs are achieved at 6.6 GHz and 8.5 GHz, respectively, which highly improve the frequency selectivity of the upper stopband. In addition, the filter enjoys a wide upper stopband from 5.0 GHz to 11.0 GHz.

### 3.2 Dual-band BPF design

To design dual-band BPF without changing the size of the filter, high-mode is adopted based on the design of the single band BPF as shown in Fig. 5.

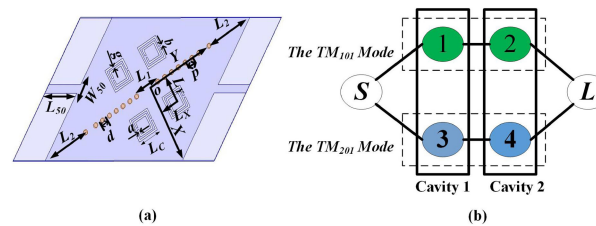


Fig. 5. (a) Structure of the dual-band BPF (b) Coupling scheme of the dual-band BPF

Another two inductive windows are loaded to fulfill  $TM_{201}$  mode coupling. By adjusting the parameter  $L_2$  appropriately, the  $TM_{201}$  mode can couple with each other while the  $TM_{101}$  mode be suppressed, then the second bandpass is achieved. However, the spurious mode ( $TM_{202}$ ) also can be coupled with each other, which will disturb the performance of the second passband. In order to solve it, by adjusting the locations of the feeds, TZs can be obtained at the middle and upper stopband, respectively. To further suppress  $TM_{202}$  mode, two pairs of CSRRs are etched on the surface of waveguide. By adjusting the positions and the sizes of CSRRs ( $L_X, L_Y, L_C$ ), the selectivity of the upper stopband can be highly improved as shown in Fig. 6(a). The final optimized dimensions are as follows (unit: mm):  $L_{50} = 4.0$ ,  $W_{50} = 1.03$ ,  $d = 0.5$ ,  $P = 1.0$ ,  $L_1 = 3.08$ ,  $L_2 = 5.95$ ,  $L_X = 2.9$ ,  $L_Y = 3.08$ ,  $L_C = 2.62$ ,  $a = 0.2$ ,  $b = 0.2$ ,  $g = 0.2$ .

In Fig. 6, two expected passbands are achieved at 4.5 GHz and 6.5 GHz, respectively. The measured insert loss and 3 dB FBW of both passbands are 2.34 dB, 200 MHz, and 2.28 dB, 400 MHz, respectively. Two TZs are obtained at 4.6 GHz and 6.6 GHz, respectively, which improve the attenuation level of the middle and the upper stopband.

Here, some comparisons between our proposed and previous dual-band SIW filters are summarized in Table II, where attenuation is between two passbands. The

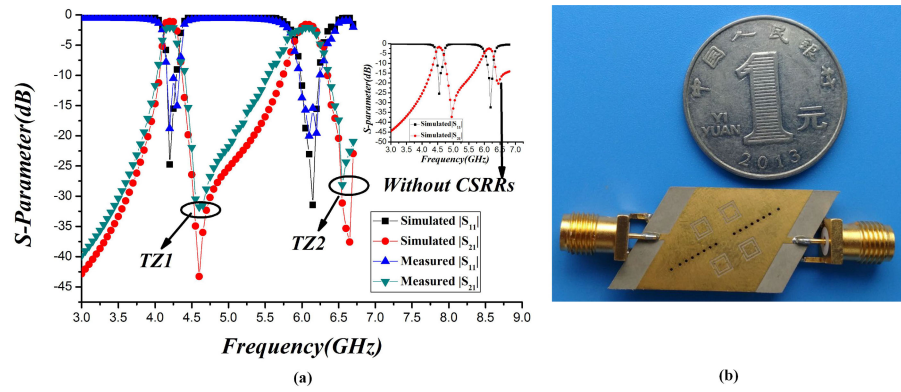


Fig. 6. (a) S-parameters (b) Photograph of the BPF

Table II. Comparisons between dual-band SIW filters

Reference	Size ( $\lambda_0 * \lambda_0$ )	Frequency Ratio	Attenuation	layers
[9]	1.98 * 1.30	1.05	Good	single-layer
[10]	0.21 * 0.18	1.63	Poor	single-layer
[11]	1.10 * 1.25	1.15	Good	double-layer
This work	0.32 * 0.65	1.46	Good	single-layer

advantages of the dual-band BPF are obvious, such as simple structure, low cost and small size.

### 3.3 Conclusion

In this paper, a novel OTMSIWR with one electric wall and two virtual magnetic walls is proposed. Based on it, a single-band filter with wide upper stopband is designed and fabricated. Then, a dual-band BPF with two TZs, simple structure and small size is proposed by using high-order mode technology. Finally, two kinds of filters are fabricated and measured. The measured results indicates that the OTMSIWR is a good candidate for designing filters.

### Acknowledgments

This work is supported by the fundamental research funds for the central universities (2015XKMS029).